

Feher Modulation 16 QAM

Patrick Jungwirth, PhD
US Army RDECOM
Aberdeen Proving Ground, MD 21005

Abstract

We present simulations of conventional quadrature amplitude modulation (QAM) and Feher-QAM to estimate the bandwidth improvement for Feher-QAM. We show more than a 10% improvement (reduction) in bandwidth for Feher-QAM over conventional QAM. We also show the power spectral density for Feher-QAM has a much faster convergence than conventional QAM.

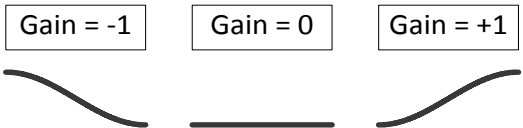
Conventional digital modulation techniques are limited by embedded rectangular windowing functions. Some more advanced modulation techniques utilize raised cosine windowing functions (filters) to improve sidelobes. Feher modulation uses a half cycle raised cosine waveform to reduce bandwidth and improve sidelobe attenuation. Feher modulation offers the equivalent power spectral density convergence of a raised cosine windowing function with twice the width (half the bandwidth). All symbol transitions in Feher modulation are smooth and occur at zero slope points. The smooth, zero slope transitions help improve intersymbol interference, and reduce timing jitter problems.

Key words: Feher modulation, QAM, Feher-QAM

1. Introduction

We present a short introduction to Feher, half cycle raised cosine, modulation. Feher modulation consists of half cycle raised cosine functions concatenated together to form a smooth function. For the symbol sequence $\{0, 1\}$ a step change occurs when transitioning from 0 to 1 in conventional modulation. In Feher modulation, the symbol transition occurs over a full symbol time. The sequence $\{0, 1\}$ is mapped to a positive going half cycle raised cosine waveform, \nearrow , with gain = +1 in (1.1). The sequence $\{1, 0\}$ is mapped to a negative going half cycle raised cosine waveform, \searrow , with gain = -1 in (1.1). The sequences $\{0, 0\}$ and $\{1, 1\}$ are mapped to a zero slope line segment, $—$, as shown by gain = 0 in (1.1).

Half Cycle Raised Cosine
(basis function)



The diagram shows three waveforms corresponding to different gain values. Above each waveform is a box containing the gain value: 'Gain = -1', 'Gain = 0', and 'Gain = +1'. The 'Gain = -1' waveform is a downward-sloping half-cycle raised cosine curve. The 'Gain = 0' waveform is a horizontal line segment. The 'Gain = +1' waveform is an upward-sloping half-cycle raised cosine curve.

(1.1)

The mapping of serial data $\{0, 1, 1, 1, 0, 0, 1\}$ to Feher modulation is illustrated in Figure 1.1. The initial symbol (condition) is assumed to be 0 . The 0^* to 0 transition is mapped to a zero slope line segment (where 0^* is the assumed initial symbol). The next symbol transition is $0 \rightarrow 1$ which is mapped to a positive going half cycle raised cosine waveform, \nearrow . The $1 \rightarrow 1$ transition is mapped to a zero slope line segment, $—$. The $1 \rightarrow 1$, $1 \rightarrow 0$, $0 \rightarrow 0$, and $0 \rightarrow 1$ mappings are also shown in Figure 1.1. As illustrated in Figure 1.1

Feher modulation is a smooth function with zero slope points occurring at the serial data symbol transition points (dashed vertical gray lines). Figure 1.1 also shows that each half cycle raised cosine waveform (gain = -1, 0, and +1) occurs over one serial data symbol time.

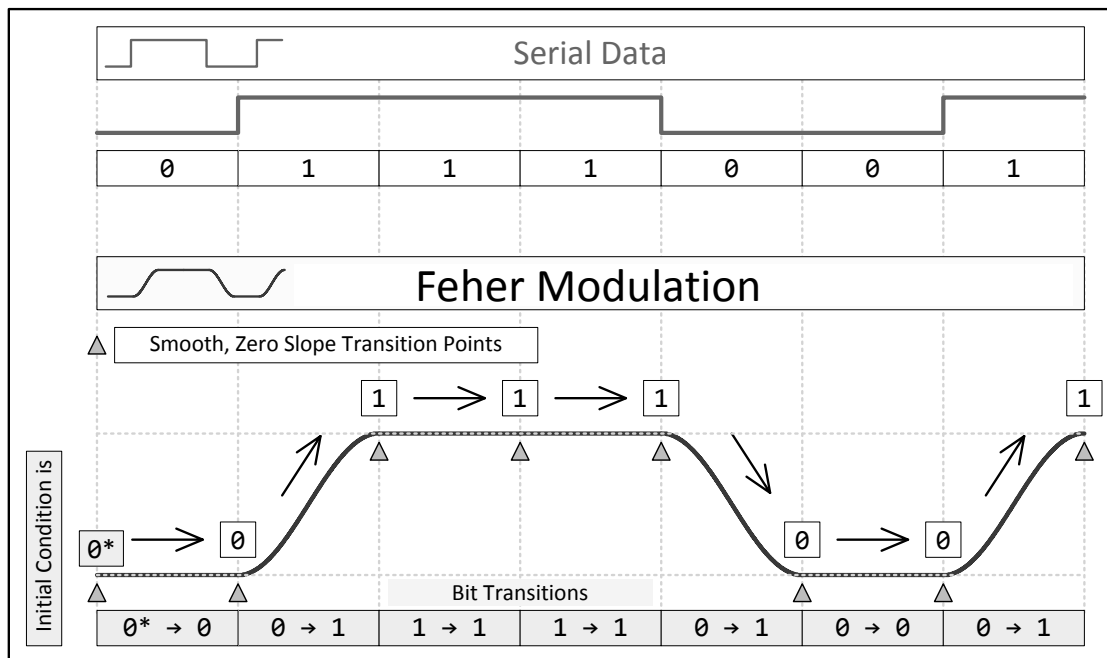


Figure 1.1. Feher Half Cycle Raised Cosine Modulation

2.0 Windowing Functions

Equation (2.1) introduces the unit step function. The unit step function is used to create the rectangular windowing function in (2.2). Equations (2.2) through (2.5) introduce a number of windowing functions. When data is sampled over a finite length of time, the resulting function is equivalent to a rectangular windowing function times an infinitely long function. The rectangular windowing function has slow (poor), $dB(f) = 20 \log \left(\frac{\sin(f)}{f} \right)$, power spectral density convergence as illustrated in Figure 2.1. To improve the convergence of sampled data, a raised cosine windowing function is used to reduce the effects of the rectangular windowing function.

For the serial data stream in Figure 1.1, the step changes embed rectangular windowing functions in the serial data's power spectral density [1-5]. From a practical point of view, Feher modulation minimizes the slope when transitioning from serial data symbol, n , to the next serial data symbol, $n+1$. Full cycle raised cosine modulation, and overlapped raised cosine modulation are described in [6-8].

The half cycle raised cosine windowing function (2.5) has the same power spectral density convergence as a raised cosine window with twice the width (2.4). In section 4, simulations are used to determine the bandwidths for conventional quadrature amplitude modulation, and Feher-QAM. We will show in sections 4 and 5 that the half cycle raised cosine windowing function results in more than a 10 % reduction in bandwidth for 16 quadrature amplitude modulation.

Unit step function, $u(t)$



$$(2.1)$$

Rectangular windowing function (width = 2)

$$w_{rec}(t) = u(t + 1) - u(t - 1)$$



$$(2.2)$$

Raised Cosine windowing function (width = 2)

$$w_{rc}(t) = \begin{cases} \frac{1+\cos 2\pi t}{2} & -1 \leq t < 1 \\ 0 & \text{otherwise} \end{cases}$$



$$(2.3)$$

Raised Cosine windowing function (width = 4)

$$w_{rc}(t) = \begin{cases} \frac{1+\cos \pi t}{2} & -2 \leq t < 2 \\ 0 & \text{otherwise} \end{cases}$$



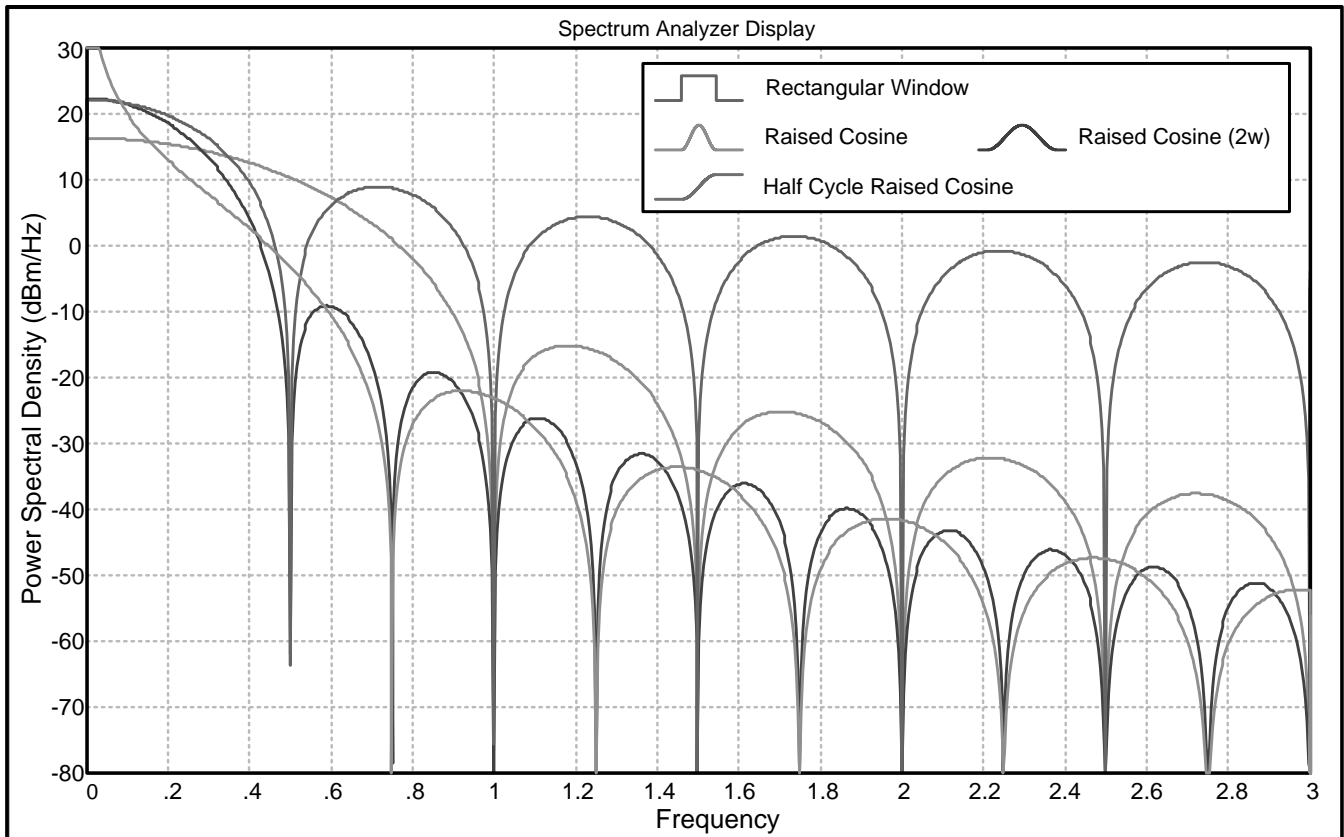
$$(2.4)$$

Half Cycle Raised Cosine windowing function

$$w_{hc}(t) = \begin{cases} \frac{1+\cos(\pi t - \frac{\pi}{2})}{2} & -1 \leq t < 1 \\ 0 & \text{otherwise} \end{cases}$$



$$(2.5)$$



3.0 Quadrature Amplitude Modulation (QAM) Background

Quadrature amplitude modulation(QAM) $I(t)$ and $Q(t)$ values are found in the diagrams in Figure 3.1 and Figure 3.2. (3.1)

$$s(t) = I(t)\cos(2\pi f_c t) - Q(t)\sin(2\pi f_c t) \quad f_c = \text{carrier frequency in Hz}$$

Equation (3.1) provides the general definition for quadrature amplitude modulation. Cosine and sine terms are multiplied by $I(t)$ and $Q(t)$ signals respectively. The term $I(t)$ is in-phase with the cosine carrier and $Q(t)$, the quadrature phase term, is 90° ($\frac{\pi}{2}$ radians) out of phase with the cosine carrier. Figure 3.1 presents the constellation diagram for 4 level QAM which is equivalent to 4 level phase modulation. We see the points on the constellation diagram all have a radius of 1 with phase angles at $\pm 45^\circ$ and $\pm 135^\circ$ ($\frac{\pm\pi}{4}$ and $\frac{\pm 3\pi}{4}$ radians). The angle sum identity shows 4 level QAM reduces to phase modulation. This is a special case; in general the I and Q terms create both amplitude and phase modulation.

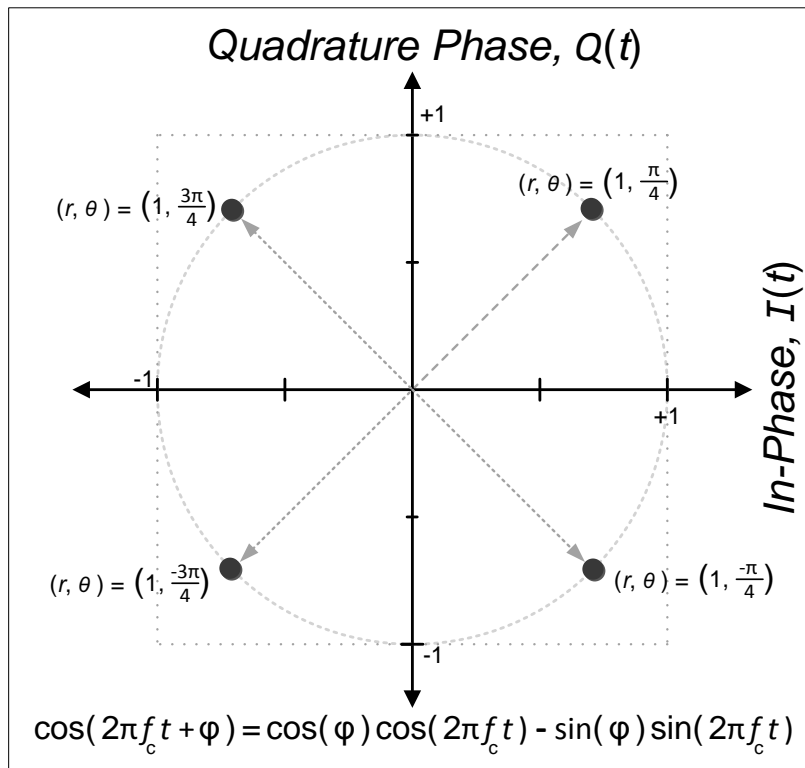


Figure 3.1. 4 Level QAM or 4 Level Phase Modulation

Message = “DSP” = 0x44; 0x53; 0x50 (where 0x## indicates a hexadecimal number) (3.1)

We present an example message = “DSP” to show how ASCII characters are converted to 16 level quadrature amplitude modulation. The message “DSP” in {3.1}, converted to ASCII code gives “D” = 0x44, “S” = 0x53, and “P” = 0x50. For 16 QAM in Figure 3.2, there are 16 symbols {0x0, 0x1, 0x2, 0x3, 0x4, 0x5, 0x6, 0x7, 0x8, 0x9, 0xA, 0xB, 0xC, 0xD, 0xE, 0xF}. Each group of 4 bits from the

message “DSP” is converted to a (I, Q) vector representation for 16 QAM modulation. Figure 3.2 shows the 4 bit code to 16 QAM look-up table. For “D”=0x44, the 4 bit groups are 0x4; 0x4, the (I, Q) vector for 0x4 is (0.75, 0.25) volts. Equation (3.2) shows the (I, Q) vector values for the message in {3.1}. The QAM signal, $s(t)$ as shown in (3.1), is calculated from the n -th (I, Q) vector and the cosine and sine carrier terms.

Figure 3.3 shows a 16 level QAM modulator block diagram and simulation. Figure 3.3 clearly shows step functions present in 16 QAM. The embedded step functions (rectangular windowing functions) result in a $\text{sinc}(x)/x$ power spectral density function as shown in Figure 3.3.

$$\begin{aligned}
 &\text{Message} = \text{“DSP”} = 0x44; 0x53; 0x50 \\
 &\text{“D”} = 0x4; \quad 0x4 \quad \text{“S”} = 0x5; \quad 0x3 \quad \text{“P”} = 0x5; \quad 0x0 \quad (3.2) \\
 (I, Q)_{(n)} = &(+0.75, +0.25), (+0.75, +0.25); (+0.25, +0.25), (-0.25, +0.75); (-0.25, +0.25), (+0.75, +0.75)
 \end{aligned}$$

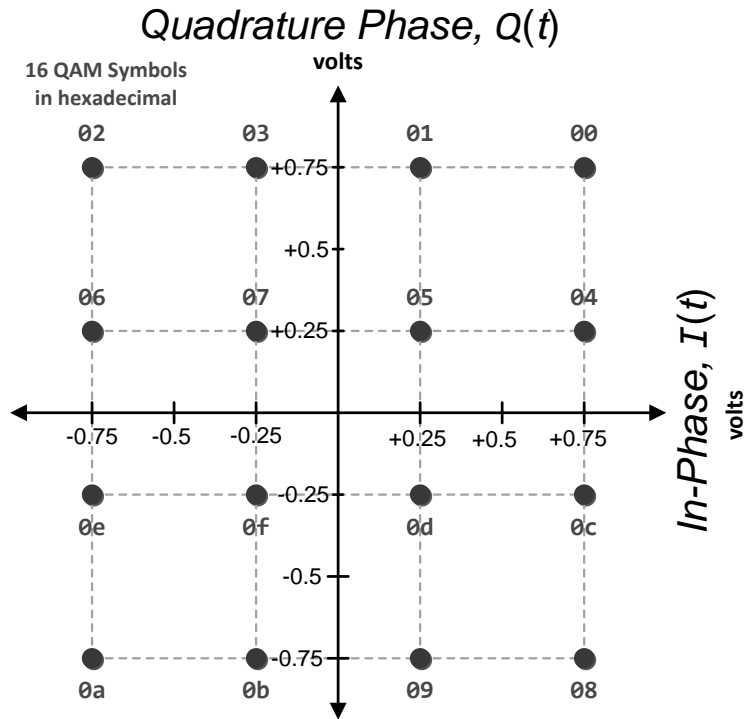


Figure 3.2. 16 QAM Constellation Diagram

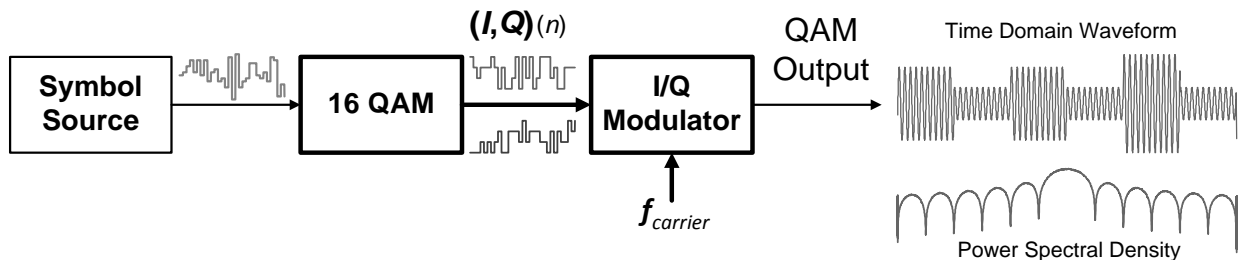


Figure 3.3. 16 QAM Modulator Block Diagram

4.0 Feher-Quadrature Amplitude Modulation (QAM)

Feher quadrature amplitude modulation (QAM) is similar to the binary example in Figure 1.1. Serial binary data consists of two amplitude values +1 and -1 (or 1 and 0). 16 QAM consists of 4 amplitude values for I and 4 amplitude values for Q . As illustrated in Figure 3.2, the 4 amplitude values are -0.75, -0.25, +0.25, and +0.75. The half cycle raised cosine functions are gain scaled by (4.1) to connect the (I, Q) QAM symbols together. For the half cycle raised cosine waveform, the initial value, $DC_Offset(n)$ in (4.2), is the final value from the previous symbol. $H_{RC}(t)$ in (4.3) generates unit amplitude, half cycle raised cosine waveforms. Feher QAM in (4.4) is a unit half cycle raised cosine, $H_{RC}(t)$ in (4.3), gain scaled by (4.1), plus the final value from the previous (I, Q) vector in (4.2).

$$\mathbf{Gain}(n) = (I, Q)_{(n)} - (I, Q)_{(n-1)} \quad (4.1)$$

$$\mathbf{DC_Offset}(n) = (I, Q)_{(n-1)} \quad (4.2)$$

$$H_{RC}(t) = \frac{1}{2} \left[\cos(2\pi f_{sym} \sigma) + 1 \right] \quad \text{Periodic Half Cycle Raised Cosine} \quad (4.3)$$


$\sigma(t) = \text{锯齿波}$ Where $\sigma(t)$ is the sawtooth function

$$\mathbf{Feher_QAM}(t) = H_{RC}(t) \cdot \mathbf{Gain}(n) + \mathbf{DC_Offset}(n) \quad (4.4)$$

Figure 4.1 shows a block diagram implementing Feher modulation algorithm for 16 QAM. Vector operations are shown as **thick lines**. Scalars are shown by thin lines. The most complicated part of Feher modulation algorithm is the unit half cycle raised cosine generator, $H_{RC}(t)$ in (4.3). The rest of the operations are vector addition and scalar multiplication. A look-up table (Figure 3.2) converts 4 bit numbers to 16 QAM symbols.

Conventional QAM and Feher QAM are compared in Figure 4.2. The half cycle raised cosine waveforms form smooth curves from $(I, Q)_{(n-1)}$ to $(I, Q)_{(n)}$. The Feher QAM waveforms are smooth functions without step changes. At each conventional QAM symbol transition, Feher QAM has a zero slope. Each half cycle raised cosine requires a full conventional QAM symbol time to change state. Figure 4.1 shows a Feher 16 QAM modulated waveform. It is a smooth function without any step changes.

Figure 4.3 and Figure 4.4 compare simulations of conventional 16 QAM to Feher 16 QAM. Figure 4.4 shows an expanded scale highlighting the main lobes. Conventional QAM has a $\sin(x)/x$ power spectral density function with a slow convergence. Feher QAM has a narrower main lobe with a much faster convergence (cosine-like windowing function). Section 5 compares bandwidth and convergence for conventional QAM and Feher-QAM.

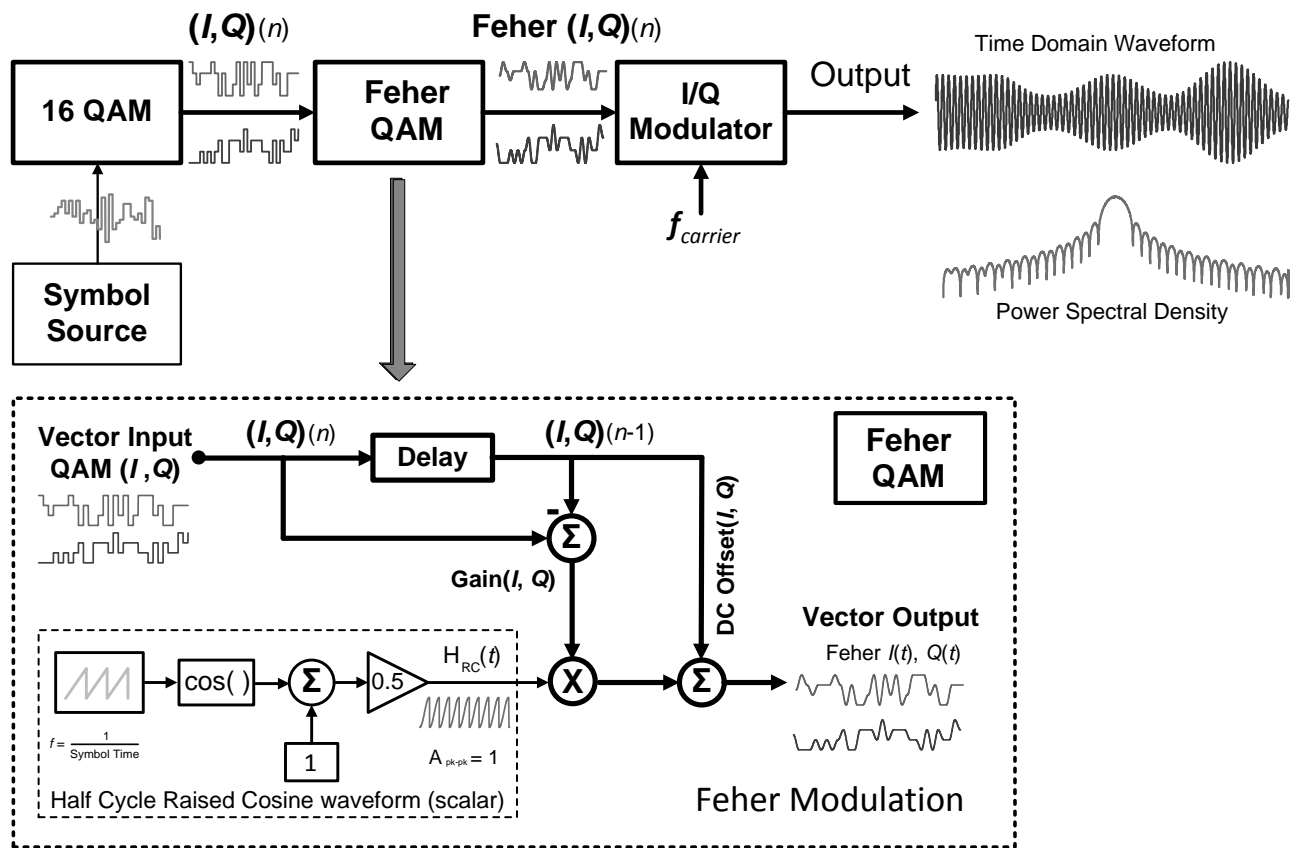


Figure 4.1. Feher-QAM Block Diagram.

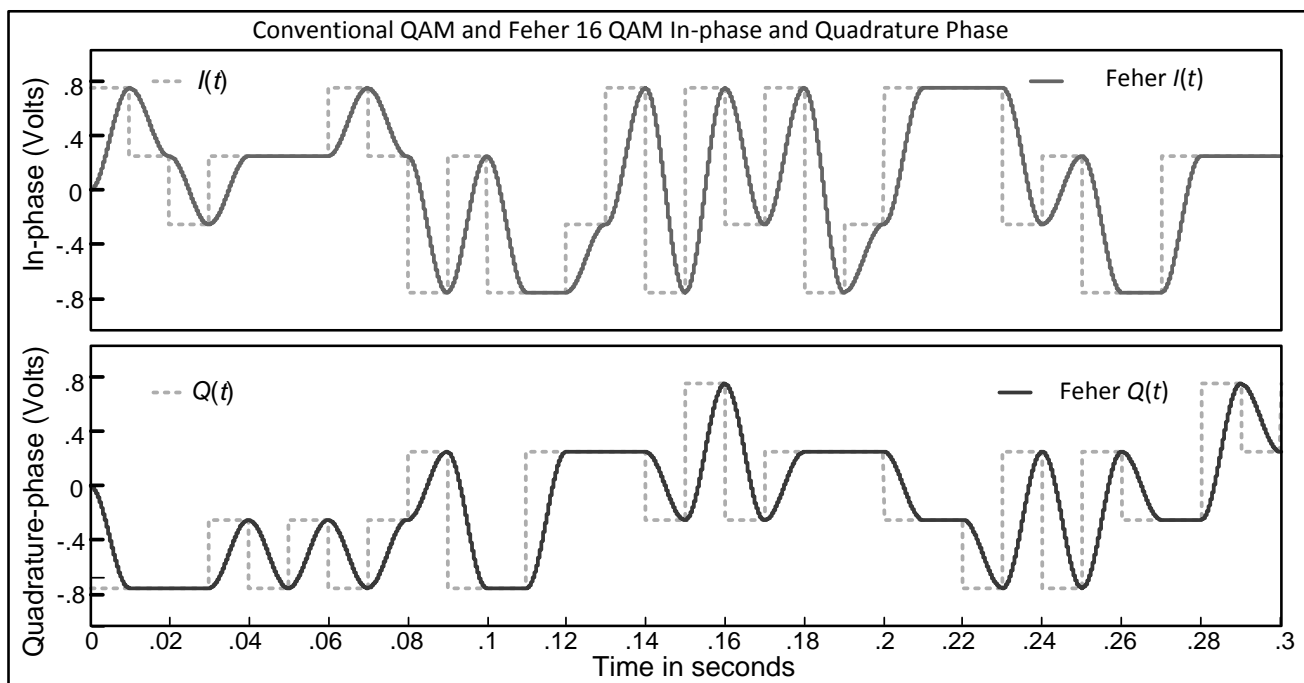


Figure 4.2. Simulated QAM and Feher QAM Waveforms

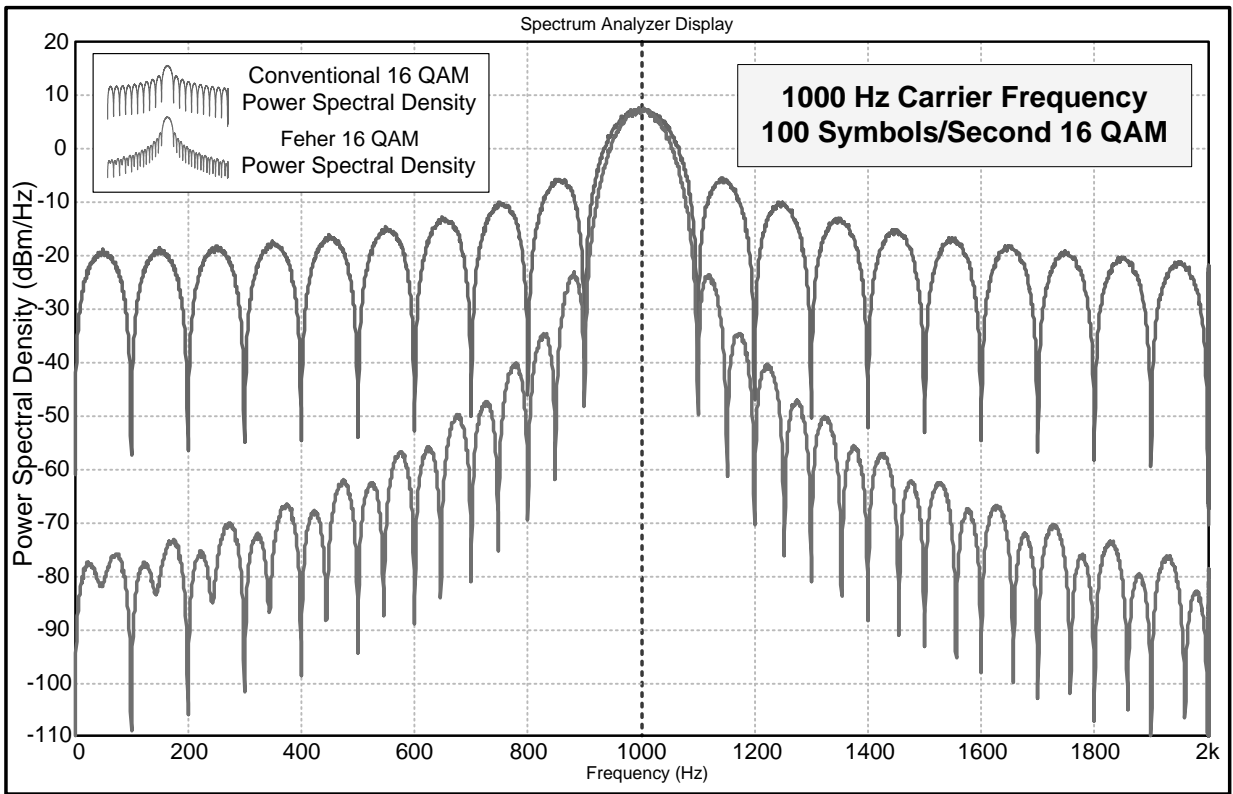


Figure 4.3. Simulated 16 QAM and Feher-QAM Power Spectral Density

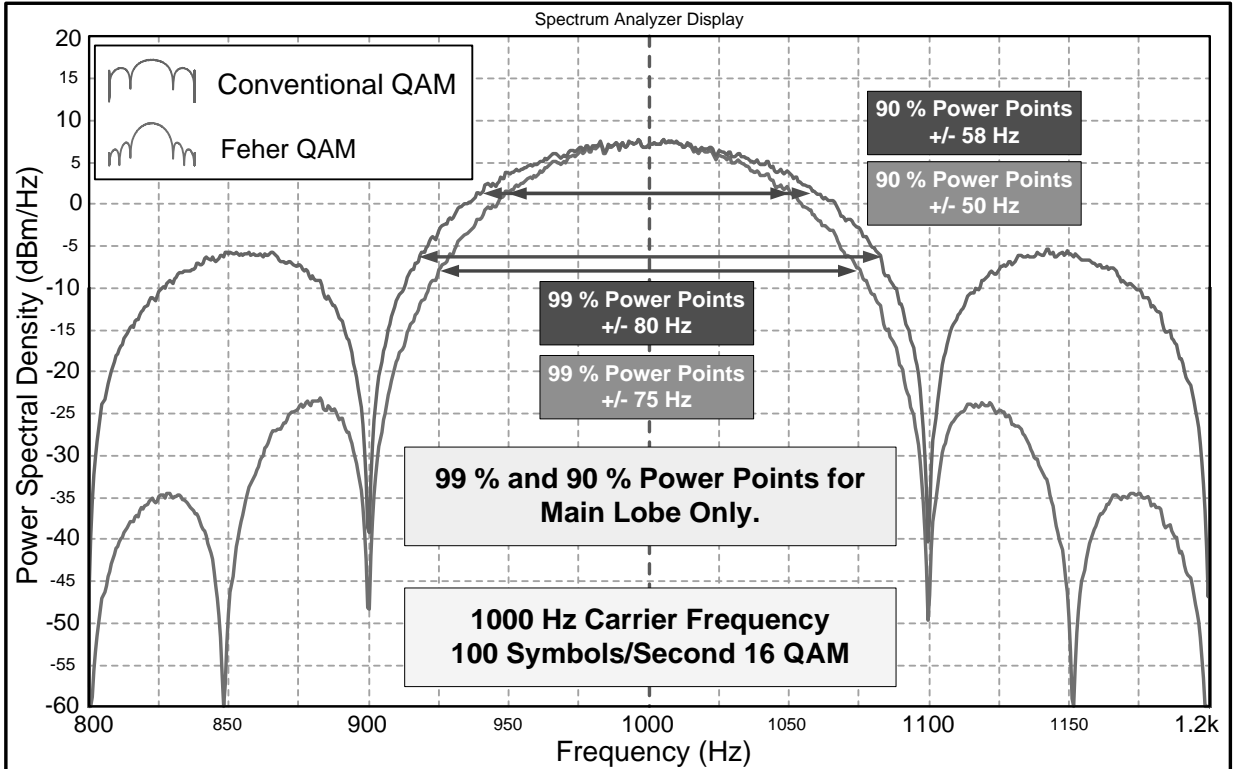


Figure 4.4. QAM and Feher-QAM 90% and 99% Power Bandwidth Points

5.0 Bandwidth Comparison

We simulated a 1000 Hz carrier frequency, 100 symbol/second conventional QAM modulator and Feher-QAM modulator using the simulation tool in [9]. Table 5.1 *only* compares power bandwidth points for the main lobes. As shown in Figure 4.4 the sidelobes for conventional QAM are much larger than Feher-QAM. Including the first sidelobes in the power bandwidth calculation would show even a *larger* improvement for Feher-QAM. Table 5.1 shows better than a 10 % improvement in the 90 % power bandwidth points for Feher-QAM. Table 5.2 shows a 30 dB improvement in power spectral density convergence at $\pm 2f_{\text{sym}}$ (2 times the symbol frequency). Tables 5.1 and 5.2, and Figures 4.3 and 4.4 show improved (reduced) bandwidth and much better convergence for Feher-QAM compared to conventional QAM.

Table 5.1. Bandwidth Points in terms of Symbol Frequency (100 Hz)

Bandwidth Points	Conventional QAM	Feher-QAM	Improvement
90 % Power Points	± 58 Hz or ± 58 %	± 50 Hz or ± 50 %	13.8 %
99 % Power Points	± 80 Hz or ± 80 %	± 75 Hz or ± 75 %	6.3 %

Table 5.2. Convergence in terms of Symbol Frequency (f_{sym})

Symbol Frequency	Conventional QAM	Feher -QAM	Improvement
$\pm 2f_{\text{sym}}$	- 7 dBm/Hz	- 37 dBm/Hz	30 dB
$\pm 4f_{\text{sym}}$	-15 dBm/Hz	-56 dBm/Hz	41 dB

6. Conclusion

We show that Feher-QAM has better than a 10% improvement in bandwidth and 30 dB improvement in power spectral density at $\pm 2f_{\text{sym}}$ (2 times the symbol frequency). Feher modulation simply adds an additional DSP stage prior to the final modulation stage as shown in Figure 4.1. Feher modulation is a general technique and can easily be applied to other digital modulation techniques.

7. Acknowledgement

The author wishes to thank RDECOM community for the opportunity to research Feher modulation.

8. Disclaimer and Copyright

Reference herein to any specific commercial, private or public products, process, or service by trade name, trademark, manufacturer, or otherwise, does not constitute or imply its endorsement, recommendation, or favoring by the United States Government. The views and opinions expressed herein are strictly those of the author(s) and do not represent or reflect those of the United States Government.

US Government work. Distribution statement A: approved for public release, distribution is unlimited.

9. References

- [1] K. Feher: "Filter," US Patent 4,339,724, July 1982.
- [2] P. Simon and T. Yan: "Performance Evaluation and Interpretation of Unfiltered Feher-Patented Quadrature-Phase-Shift Keying (FQPSK)," NASA TMO Progress Report 42-137 May 15, 1999.
http://ipnpr.jpl.nasa.gov/progress_report/42-137/137C.pdf.
- [3] M. Simon and D. Divsalar: "Further Results on a Reduced-Complexity, Highly Power/Bandwidth-Efficient Coded Feher-Patented Quadrature-Phase-Shift-Keying System with Iterative Decoding," NASA IPN Progress Report 42-146, August 15, 2001. http://tmo.jpl.nasa.gov/progress_report/42-146/146I.pdf
- [4] P. Jungwirth: "SSTM," AlaSim International Conference and Exposition," Huntsville, Alabama, 6 – 7 May 2014. <http://www.almc.org/alasim-international.shtml>
- [5] P. Jungwirth: "SSTM," TAPR Conference, Austin TX, pp. 32-51, September 5-7, 2014.
<https://www.tapr.org/pdf/DCC2014-SmoothedSymbolTransitionModulation-Patrick-Jungwirth.pdf>
- [6] G. Lili, et al.: "Symmetric Raised Cosine Keying Modulation and Performance Analysis," IEEE International Conference on Computer Science and Network Technology, pp. 88-91, Dec. 2011.
- [7] M. Simon, et al.: "Trellis-Coded Quadrature-Phase-Shift Keying (QPSK) With Variable Overlapped Raised-Cosine Pulse Shaping," NASA TMO Progress Report 42-136, February 15, 1999.
ipnpr.jpl.nasa.gov/progress_report/42-136/136F.pdf
- [8] M. Austin, and M. Chang: "Quadrature Overlapped Raised Cosine Modulation," IEEE Transactions on Communications Theory, Vol. Com-29, No. 3, pp. 236-249, March 1981.
- [9] Visual Solutions: Vissim/Comm, www.vissim.com.